Isomeric yield ratios and excitation functions in α-induced reactions on ^{107,109}Ag

R. Guin and S. K. Saha
Radiochemistry Division, Bhabha Atomic Research Centre, Variable Energy Cyclotron Centre, I/AF Bidhan Nagar, Calcutta-700 064, India

Satya Prakash*
Radiochemistry Division, Bhabha Atomic Research Centre, Bombay-400 085, India

M. Uhl
Institut für Radiumforschung und Kernphysik, Universität Wien, A-1090 Vienna, Austria
(Received 31 December 1991)

Isomeric yield ratios for the reactions ^{107}Ag$(\alpha,3n)^{108}$In, ^{107}Ag$(\alpha,\alpha3n)^{104}$Ag, ^{109}Ag$(\alpha,2n)^{111}$In, and ^{109}Ag$(\alpha,3n)^{110}$In are determined in the energy range of 20–63 MeV α particles. Excitation functions for the above reactions as well as for the ^{107}Ag$(\alpha,2n)^{109}$In, ^{107}Ag$(\alpha,\alpha2n)^{105}$Ag, ^{109}Ag$(\alpha,4n)^{109}$In, ^{109}Ag$(\alpha,5n)^{108}$In, and ^{109}Ag$(\alpha,\alpha4n)^{105}$Ag reactions are also presented. Experimental excitation functions are compared with statistical model calculations taking into account precompound particle emission. Isomeric yield ratios are found to depend strongly on the root mean square orbital angular momentum in the entrance channel. A semiempirical method for the prediction of isomeric yield ratios failed to reproduce experimental data even for compoundlike reactions. Isomeric yield ratios were also calculated in the frame of a statistical model under consideration of angular momentum effects in the preequilibrium and the equilibrium stage. Overall agreement between the theory and the experiment for isomeric yield ratios was found to be satisfactory especially at low bombarding energy when compound nucleus reaction channel is dominant. The discrepancy observed at higher bombarding energies needs to be theoretically investigated in greater detail.

PACS number(s): 25.55.−e, 27.60.+j

I. INTRODUCTION

Nuclear reactions induced by medium energy projectiles (10–30 MeV/nucleon) are dominated by the preequilibrium and equilibrium deexcitation processes. The highly excited nuclear system formed by the bombardment of energetic charged particles deexcites first by the emission of fast nucleons at the preequilibrium stage and then the system cools down by the emission of light particles (mostly neutrons in our case with compound system $Z=49$) at the equilibrium stage. As the excitation energy of the compound system decreases (<10 MeV), deexcitation by the emission of statistical γ rays predominates, leading to the population of the residual nucleus either in its ground state or in its low-lying isomeric state.

Several models [1–3] have been proposed to calculate excitation functions and energy spectra of light particles emitted by the equilibrium/preequilibrium processes. Theoretical predictions are found to agree reasonably well with experimental excitation functions [4–6] for $(\alpha,xnyp)$ reactions. There are many data on the energy spectra of light ejectiles and the excitation functions for light particle (^{4}He, ^{3}He, p, etc.) induced nuclear reactions, but information on the yield ratios of high spin state to low spin state (σ_{HS}/σ_{LS}) of a residual nucleus and their dependence on the incident particle energy is far from abundant. A study of the isomeric yield ratios in nuclear reactions provides useful information regarding the level density and discrete level structure of the residual nucleus [7–10]. The measurement of σ_{HS}/σ_{LS} is also useful for the estimation of the amount of angular momentum transferred in the entrance channel over a wide range of the incident projectile energy [11–13].

The present paper is aimed at looking into the effect of the entrance channel angular momentum and the preequilibrium particle emission on the relative population of the isomeric and ground states of a residual nucleus. In this paper we present the experimental isomeric yield ratios for (α,xn) and $(\alpha,\alpha xn)$ reactions on ^{107,109}Ag. The dependence of the σ_{HS}/σ_{LS} on the energy of the incident particle and on the entrance channel angular momentum is discussed. Excitation functions for the ^{107}Ag$(\alpha,2n)$, ^{107}Ag$(\alpha,3n)$, ^{109}Ag$(\alpha,2n)$, ^{109}Ag$(\alpha,3n)$, ^{109}Ag$(\alpha,4n)$, ^{109}Ag$(\alpha,5n)$, ^{107}Ag$(\alpha,\alpha2n)$, ^{107}Ag$(\alpha,\alpha3n)$, and ^{109}Ag$(\alpha,\alpha4n)$ reactions have also been measured and compared with theoretical model calculations [14]. Recently, the code MAURINA [15], based on compound nucleus evaporation for equilibrium decay and the exciton model for preequilibrium emission, has been developed and the present results are compared with the model calculations to test the adequacy of the underlying physics.

II. EXPERIMENTAL PROCEDURES

Excitation functions and isomeric yield ratios for α-induced reactions on ^{107,109}Ag were obtained by the

*Present address: Chemistry Department, Dayalbagh Educational Institute, Agra, India.

stacked-foil technique. For the measurement of isomeric yield ratios, targets of about 1 mg/cm^2 were prepared by vacuum evaporation of natural silver on 6.8 mg/cm^2 aluminum backing. The target assembly consisted of a number of silver targets sandwiched between aluminum degrader foils. The thickness of the degrader foils was adjusted so as to get the desired beam energy on different targets. The stopping power data of Williamson, Boujot, and Pickard [16] were used to calculate the beam energy degradation in each foil. For excitation function measurements, 26.6-mg/cm^2-thick natural silver foils were used.

Irradiations were carried out in the energy range of 20–63 MeV α-particles at the Variable Energy Cyclotron Centre (VECC), Calcutta. The beam energy resolution of the unanalyzed beam at VECC is about 0.2 MeV. The total energy degradation of the α-beam in our target assembly never exceeded 15 MeV. The uncertainty in absolute energy of the beam falling on different targets can be expected to be ≤ 1.5 MeV. The uncertainty in the projectile energy is due to the energy spread of the incident beam from the cyclotron and energy loss straggling. For excitation function measurements, irradiations were carried out for 10 min with a beam current of about 100 nA. For the isomeric yield ratio measurements, the beam current was about 750 nA and the duration of irradiation was varied from 10 min to 1 h depending on the half-lives of the products of interest. The average beam current passing through the target stack was measured by a Faraday cup. In addition, a 6.8-mg/cm^2-thick aluminum monitor foil was used in each stack. Cross sections for the ^{27}Al$(\alpha,5n4p)^{22}$Na and ^{27}Al$(\alpha,3n4p)^{24}$Na reactions are well known [17]. The reliability of the charge measurement using the Faraday cup was always cross-checked from the yields of ^{22}Na and ^{24}Na produced by the α-induced reaction on ^{27}Al.

Gamma rays emitted by the activated foils were monitored using a 10% HPGe detector. The detector resolution was found to be 1.9 keV at 1333 keV ^{60}Co peak. Energy and efficiency calibrations of the detector were performed using ^{152}Eu standard sources. The irradiated samples were always positioned at fixed geometry at a distance of 20 cm or more from the detector so as to minimize the deadtime effect. Gamma spectra were recorded in Canberra Series 88 multichannel analyzer and stored on magnetic tapes for later off-line analysis. For ^{104,105}Ag isotopes, γ spectrometry was carried out after an appropriate radiochemical separation [18].

The cross section for a given reaction was evaluated from the sum of activities of the product nuclei observed in the target and catcher foil. Nuclide identification was based on the measurement of γ-ray energy and half-life. Table I shows the spectroscopic data [19] used for the yield calculation. Only those γ rays which were used for the calculation are listed in the table. It was observed that the decay data of ^{104}Ag^{m,g} could not be explained on the basis of the reported value of 33% isomeric transition (IT) branch in the decay of ^{104}Ag^m. Therefore the decay of ^{104}Ag^m was reexamined [18] and the value of 0.07% as obtained for the IT branch of ^{104}Ag^m was used for the cross section and isomeric yield ratio calculations.

TABLE I. Spectroscopic data [19] for $^{108-111}$In and ^{104,105}Ag. The high spin and low spin states of the nuclides are represented by HS and LS, respectively.

Nuclide	Half-life	J^π	E_γ (keV)	I_γ(%)
^{108}In (HS)	58.0 min	$(5,6^+)^a$	242.8	38.4
			633.1	99.7
			875.5	94.4
^{108}In (LS)	40.0 min	3^{+a}	632.9	76.1
^{109}In (HS)	4.2 h	$\frac{9}{2}^+$	203.3	74.0
^{110}In (HS)	4.9 h	7^+	641.7	26.8
			657.7	98.5
			884.7	94.8
			937.5	69.4
^{110}In (LS)	69.0 min	2^+	657.5	97.9
^{111}In (HS)	2.83 d	$\frac{9}{2}^+$	171.3	87.6
			245.4	94.2
^{111}In (LS)	7.6 min	$\frac{1}{2}^-$	537.0	87.0
^{104}Ag (HS)	69.0 min	5^+	555.8	92.0
			767.5	65.8
			941.6	23.0
^{104}Ag (LS)	33.0 min	2^+	555.8	60.0
^{105}Ag (LS)	41.3 d	$\frac{1}{2}^-$	280.4	31.1
			344.5	42.7

[a]In the MAURINA calculations $J_{HS}=7^+$ and $J_{LS}=2^+$ have been considered for the nuclide ^{108}In [D. Vandeplassche *et al.*, Nucl. Phys. **A396**, 115 (1983); Phys. Rev. Lett. **57**, 2641 (1986)].

The activities of the irradiated foils were monitored as a function of time. From the observed activities of the isomeric and ground states of product nuclei, total cross sections and isomeric yield ratios were computed using standard radioactive decay laws [18,20].

III. RESULTS

In Tables II and III experimental results for the production of various residual nuclei formed by the α-induced reaction on ^{107}Ag and ^{109}Ag, respectively, are summarized. Their absolute uncertainties are in most cases around 10%. The error includes contributions from the counting statistics and peak integration ($\leq 4\%$), detector efficiency (5%), beam current integration (6%), and target thickness (5%), but not those of the spectroscopic data used in the analysis. The uncertainty in the beam energy has already been indicated to be ≤ 1.5 MeV. The nuclide ^{109}In can be produced by both the $(\alpha,2n)$ and $(\alpha,4n)$ reactions on ^{107}Ag and ^{109}Ag, respectively. In the overlapping region the contribution of each channel has been taken as proportional to its theoretical estimate [14]. A similar correction has also been applied to the yields of ^{108}In and ^{105}Ag. These points are indicated by an asterisk.

Some experimental cross section data of α-induced reactions on ^{107,109}Ag exist in the literature [21–24]. The agreement between the present work and previous measurements is found to be quite satisfactory in the overlapping region, but the cross section values of Wasilevsky, De la Vega Vedoya, and Nassif [24] at the low energy region of each reaction were found to differ significantly

TABLE II. Experimental cross sections (in millibarns) for the α-induced reactions on ^{107}Ag.

E_α (MeV)	Product nucleus ^{109}In	^{108}In	^{105}Ag	^{104}Ag
20.0	203.0±19.3			
24.7	815.7±65.3			
29.0	996.6±69.8			
32.9	768.8±63.0	256.3±23.1	2.3±0.4	
36.5	357.5±32.2*	476.8±39.6	19.8±2.9	
39.6	45.3±6.8*	714.2±57.1	64.5±8.4	
42.2	22.2±3.6*	918.3±64.3	103.4±10.3	
45.2		666.6±53.3	136.9±13.0	
48.3		462.5±39.3*	131.6±13.1	29.1±4.4
50.6		229.8±20.7*	131.9±13.2	41.0±5.7
53.2		93.4±10.3*	111.7±12.3*	75.8±8.3
55.9		47.3±6.6*	42.4±5.5*	118.3±11.8
58.4			18.9±2.8*	164.8±15.6

from other measurements.

For isomeric yield ratio measurements, the activities of the isomeric and corresponding ground states were determined from the same irradiation. Therefore uncertainties due to the charge integration and nonuniformities in target thickness did not contribute to the error in the determination of the isomeric yield ratio. Counting statistics, γ-peak analysis ($\leq 8\%$), and detector efficiency (5%) contribute mainly to the uncertainties in the isomeric yield ratio measurements, and the overall uncertainties are estimated to be $\leq 14\%$. The overall error in isomeric yield ratios was obtained by compounding the uncertainties in the measurements of low spin and high spin yields of an isotope. For isomeric yield ratio measurements, the range of energy of the α particles was selected such that either ^{107}Ag or ^{109}Ag present in the natural target can mainly contribute to the product of interest. Therefore no correction was necessary because of the presence of the other isotope in the natural silver target.

A systematic study of the isomeric yield ratio over a wide range of bombarding energy is lacking. Fukushima *et al.* [21,22] measured isomer ratios of ^{108}In and ^{110}In produced by $(\alpha,3n)$ reactions on ^{107}Ag and ^{109}Ag, respectively, but uncertainties associated with those measurements were very large. Misaelides and Munzel [23] also measured the isomeric yield ratios of ^{108,110}In and ^{104}Ag. In the cases of indium isotopes, isomer ratios were measured for only a few bombarding energies. For ^{104}Ag their isomer ratios as a function of bombarding energy show a similar trend as that of the present measurement, but their values of σ_{HS}/σ_{LS} differ appreciably from our data. Bishop, Huizenga, and Hummel [9] reported isomeric yield ratios of ^{110}In produced by the $(\alpha,3n)$ reaction on ^{109}Ag in the energy range of 27.5–38.6 MeV of α particles. The agreement between the present work and their measurement is reasonably good. Wasilevsky, De la Vega Vedoya, and Nassif [25] also reported the isomeric yield ratios of ^{110}In and ^{108}In produced by α-induced reactions on ^{109}Ag and ^{107}Ag, respectively, in the energy region of 30–54 MeV. However, their results differ significantly from all other measurements. Experimental isomeric yield ratios for the ^{107}Ag$(\alpha,3n)^{108}$In, ^{107}Ag$(\alpha,\alpha 3n)^{104}$Ag, ^{109}Ag$(\alpha,2n)^{111}$In, and ^{109}Ag$(\alpha,3n)^{110}$In reactions are shown in Table IV.

TABLE III. Experimental cross sections (in millibarns) for the α-induced reactions on ^{109}Ag.

E_α (MeV)	Product nucleus ^{111}In	^{110}In	^{109}In	^{108}In	^{105}Ag
20.0	451.2±36.1				
24.7	1057.9±74.1				
29.0	1110.1±77.7	178.8±16.9			
32.9	642.9±48.2	639.2±51.1			
36.5	293.9±25.0	913.1±63.9	46.0±6.9*		
39.6	144.6±13.7	985.0±68.9	254.0±22.8*		
42.2	98.7±9.9	848.8±59.4	409.8±32.8*		
45.2	73.4±8.1	605.5±48.4	617.1±49.4		
48.3	61.5±8.0	441.6±37.5	689.9±51.7	69.2±9.7*	
50.6		359.7±30.6	708.5±49.6	261.0±33.9*	
53.2		258.5±23.3	809.0±56.6	285.8±34.3*	10.8±2.1*
55.9		188.3±17.5	752.2±54.2	319.8±32.8*	59.1±8.3*
58.4		141.1±13.4	617.0±49.4		82.7±9.9*

TABLE IV. Experimental isomeric yield ratios (σ_{HS}/σ_{LS}) for ^{108}In, ^{110}In, ^{111}In, and ^{104}Ag.

E_α (MeV)	Product nucleus ^{108}In	^{110}In	^{111}In	^{104}Ag
19.8			8.8±0.99	
22.7			10.0±1.06	
25.3			17.5±1.75	
27.7		3.1±0.43	22.7±2.25	
30.1			36.4±3.60	
31.1	1.9±0.24	3.1±0.39		
32.3		3.6±0.41	39.1±4.14	
34.3	4.5±0.54	4.6±0.49	41.9±4.73	
35.3		6.2±0.66		
37.3	5.7±0.64	7.0±0.70		
40.1	6.2±0.70	10.7±1.10		
42.8	7.7±0.76	13.0±1.30		
45.2	9.0±1.02	14.0±1.58		
47.6	6.2±0.74	16.4±1.97		
49.2	5.2±0.66	16.1±1.93		
51.3		14.2±1.80		
52.7				6.4±1.09
53.6		10.3±1.34		
54.2				7.3±1.02
55.9				9.5±1.33
57.3				10.4±1.35
58.0				9.8±1.18
59.3				11.1±1.22
61.9				11.1±1.21
63.4				10.3±1.33

The present measurement has been carried out over a wide energy range so as to study the effect of entrance channel angular momentum and preequilibrium particle emission on the relative population of different spin states of a residual nucleus.

IV. DISCUSSION

Experimental excitation functions for the reactions ^{107,109}Ag(α,2n), ^{107,109}Ag(α,3n), ^{109}Ag(α,4n), and ^{107}Ag(α,α2n) are compared with theoretical calculations based on a hybrid model [26] using the program ALICE 85/300 [14]. Since the theoretical discussion for this code has been described in detail elsewhere [1,14,26–30], we briefly summarize the options used for the present calculations. Besides evaporation of n and p, emission of clusters such as d and α particles were considered in the present calculation. The nuclear masses were calculated using the Myers-Swiatecki mass formula [31]. The level density parameter was taken as $A/9$ MeV^{-1}. In the hybrid model option of ALICE 85/300, the initial exciton configuration and mean free path multiplier (k) were varied as free parameters so as to obtain the best agreement with experimental data. Figure 1(a) clearly shows that the initial exciton configuration of $n_0=4$ ($n_p=2$, $n_n=2$, and $n_h=0$), which is equivalent to a breakup of the incident α particle in the field of the nucleus, gives much better agreement than other choices such as $n_0=6$ ($n_p=2$, $n_n=3$, and $n_h=1$) or $n_0=6$ with $n_p=3$, $n_n=2$, and $n_h=1$, etc. In all subsequent calculations shown in Figs. 1(b), 2, and 3, the exciton number of $n_0=4$ has been kept constant. The mean free path multiplier (k), which accounts for the transparency of nuclear matter in the low density nuclear periphery, has only been used as a free parameter to fit experimental cross sections. Figures 1–3 indicate that the choice of $k=1$ is acceptable for all the reactions studied here.

The comparisons of experimental excitation functions with theoretical estimates are displayed in Figs. 1–3. Theoretical values are multiplied by a factor so as to match the experimental result with the theoretical value at the peak cross section point. The values of the normalizing factor (N) indicate the quality of fit between experimental and theoretical values. Experimental and theoretical α energies corresponding to the maximum cross sections for all these reactions agree within ±3.5 MeV. Since the uncertainty in the experimental beam energy

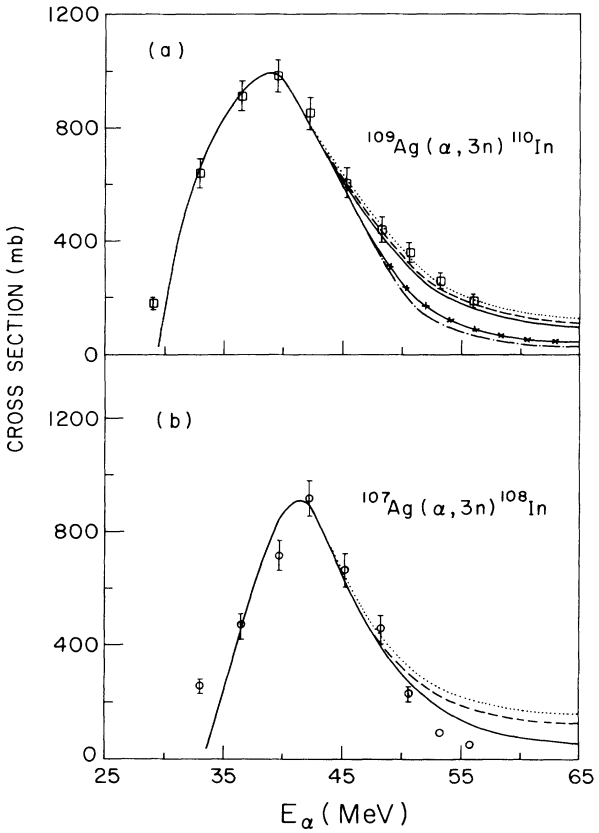

FIG. 1. Excitation functions for reactions ^{109}Ag(α,3n)^{110}In and ^{107}Ag(α,3n)^{108}In. Squares and circles represent the experimental data. (a) Dot-dashed line is the hybrid model calculation [14] with $n_0=6$ ($n_n=2$, $n_p=3$, and $n_h=1$), $k=1.0$, and $N=0.77$: cross-dashed line is the hybrid model calculation with $n_0=6$ ($n_n=3$, $n_p=2$, and $n_h=1$), $k=1.0$, and $N=0.77$; solid line is the hybrid model calculation with $n_0=4$ ($n_n=2$, $n_p=2$, and $n_h=0$), $k=1.0$, and $N=0.88$; dashed line is with $k=1.5$ and $N=0.93$; and dotted line is with $k=2.0$ and $N=0.98$. (b) Solid line is the hybrid model calculation with $n_0=4$ ($n_n=2$, $n_p=2$, and $n_h=0$), $k=1.0$, and $N=1.08$; dashed line is with $k=1.5$ and $N=1.16$; and dotted line is with $k=2.0$ and $N=1.23$.

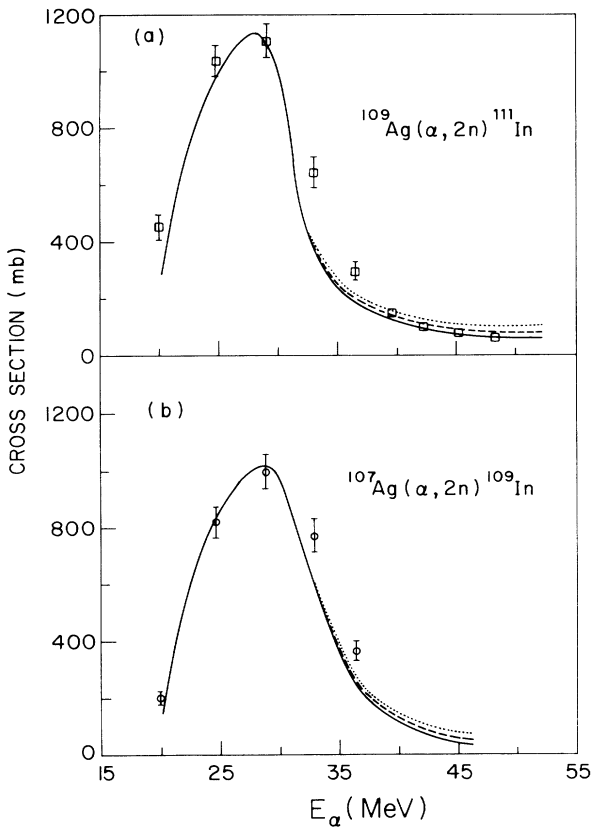

FIG. 2. Excitation functions for reactions ^{109}Ag(α,2n)^{111}In (□) and ^{107}Ag(α,2n)^{109}In (○). The details of calculation are the same as for Fig. 1(b) except for the values of N. The values of N are (a) 1.09, 1.10, and 1.11 and (b) 0.92, 0.94, and 0.95.

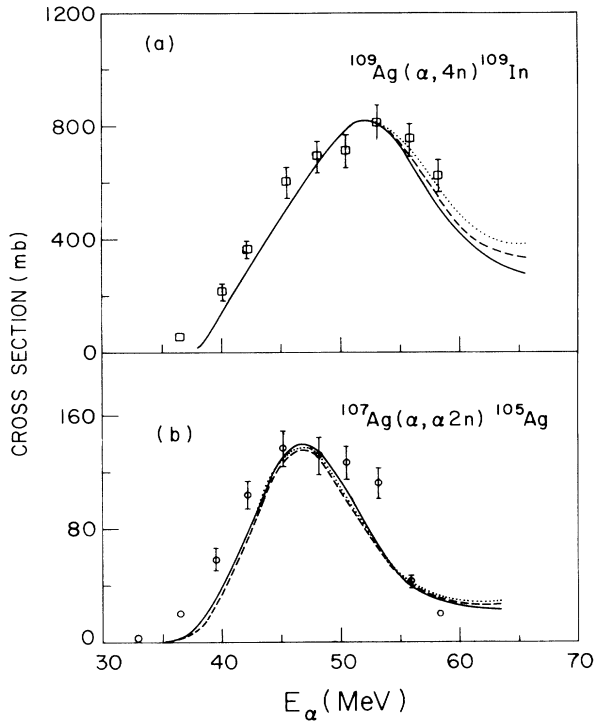

FIG. 3. Excitation functions for reactions ^{109}Ag(α,4n)^{109}In (□) and ^{107}Ag(α,α2n)^{105}Ag (○). Other details are the same as in Fig. 1(b), but the values of N are (a) 1.09, 1.22, and 1.34 and (b) 2.71, 3.00, and 3.36.

was as high as ±1.5 MeV, the agreement can be considered to be quite satisfactory. Except for the ^{107}Ag(α,α2n)^{105}Ag reaction, the value of N lies in the range of 0.9–1.3. Considering the multitudes of uncertainties in the preequilibrium calculations such as in parameters in the inverse reaction cross section, level densities, etc., the overall agreement observed between theory and experiment is remarkable.

However, Fig. 3(b) shows a large discrepancy between theory and experiment for the reaction ^{107}Ag(α,α2n)^{105}Ag. The normalizing factor for the best fit is 2.71, which is much higher than all other reactions. One might argue that the uncertainty in the estimation of the production of ^{105}Ag by the (α,α4n) reaction on ^{109}Ag may be responsible for the discrepancy. However, from our data (Table III), it is evident that the contribution of ^{105}Ag from the ^{109}Ag(α,α4n)^{105}Ag reaction is negligible up to 53.2 MeV, but the theory is unable to reproduce the shape of the excitation function even at the lower energy region. Perhaps a different reaction mechanism is playing a significant role in this reaction. Preequilibrium complex particle emission, as has been observed in several reactions [3,32], might help in reproducing the experimental data. However, such a process has not been included in the present version of the ALICE code.

Since the effect of angular momentum in the deexcitation process of particle and γ emission leading to the population of final residual nucleus is not calculated rigorously in the ALICE code, the isomeric yield ratio cannot be predicted by it directly. The initial spin distribution of the compound system resulting from the interaction of the incident α particles with the target nucleus can be calculated using Blann's model [14]. As it is known that the angular momenta carried away by the evaporated particles and statistical γ rays emitted from the compound system are usually small, the overall spin distribution of the system does not alter significantly during its deexcitation. Hence it can be expected that the isomeric yield ratio might be strongly dependent on the initial spin distribution of the compound nucleus. Figure 4 shows the dependence of the experimental isomeric yield ratio on the root mean square angular momentum ($l_{\rm rms}$), in the entrance channel. The $l_{\rm rms}$ values were calculated using the optical model and parabolic potential subroutines of the ALICE code. It is evident that the isomer ratios are strongly dependent on $l_{\rm rms}$ and not much on the spin difference of the isomer pairs, the number of neutrons emitted, or the final nuclide. In the cases of ^{108,110}In, the decrease in the values of $\sigma_{\rm HS}/\sigma_{\rm LS}$ at $l_{\rm rms} \geq 16$ (i.e., at higher bombarding energies) is due to the onset of a nonequilibrium process. It is known [1] that preequilibrium particles can carry a significant amount of angular momentum from a system, resulting in preferential population of low spin isomers. The decrease in isomeric yield ratios in ^{109}In could not be observed be-

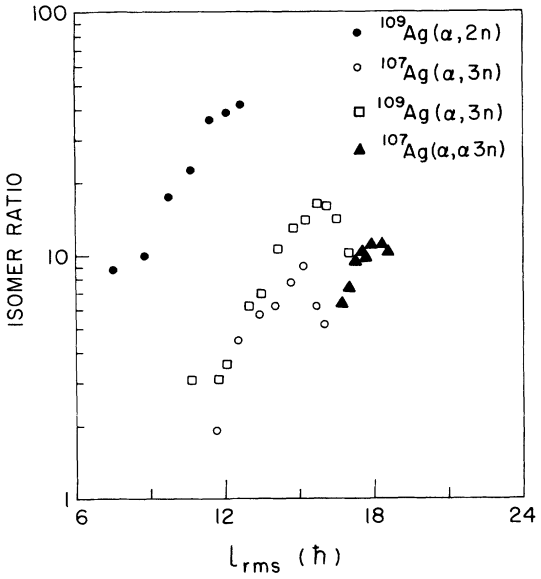

FIG. 4. Relationship between the isomeric yield ratio and the root mean square orbital angular momentum (l_{rms}) in the entrance channel for reactions ^{109}Ag$(\alpha,2n)^{111}$In, ^{109}Ag$(\alpha,3n)^{110}$In, ^{107}Ag$(\alpha,3n)^{108}$In, and ^{107}Ag$(\alpha,\alpha 3n)^{104}$Ag. The l_{rms} values were calculated using the optical model subroutines of the ALICE code [14].

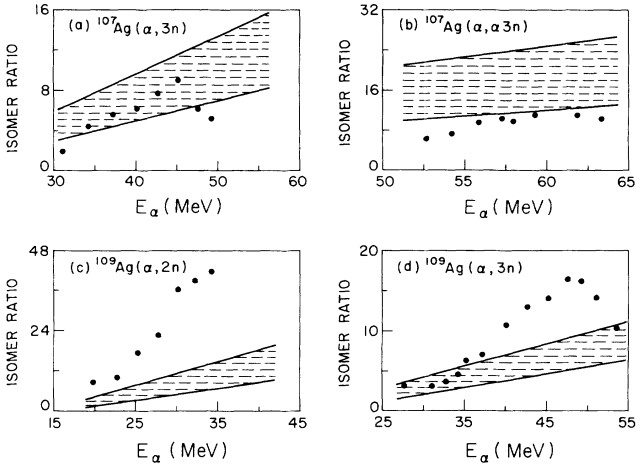

FIG. 5. Isomeric yield ratios as a function of projectile energy. Solid circles describe the experimental data. The lower and upper limits of the shaded regions are theoretical isomer ratios calculated by Blann's model [14] using the values $J_{crit}=J_{HS}+1$ and $J_{crit}=J_{HS}-1$, respectively.

cause of the lack of data at higher bombarding energies. Isomeric yield ratios in the $(\alpha,\alpha 3n)$ reaction (product nucleus ^{104}Ag) exhibit very little l_{rms} dependence, which is quite different from those of other reactions. This probably indicates the nonequilibrium or directlike emission of particles in this reaction. Similar phenomena were also observed [12] in the $(\alpha,\alpha n)$ reaction on ^{85}Rb.

It is evident from Fig. 4 that the isomeric yield ratio strongly depends on the initial spin distribution of the compound nucleus. From the predicted [14] spin distribution of the compound nucleus, isomeric yield ratios have been calculated. In this calculation it has been assumed [11,12] that all states with $J \geq J_{crit}$ populate the high spin isomer, while states with $J < J_{crit}$ deexcite to the low spin isomer. Since the J_{crit} value can be expected to be close to J_{HS}, isomer ratios were calculated in the limits $J_{crit}=J_{HS}\pm 1$, and the results are shown as the shaded regions of Fig. 5. For the reaction ^{107}Ag$(\alpha,3n)^{108}$In, the calculated σ_{HS}/σ_{LS} values agree well with the experimental data. However, for other reactions, experimental values are found to fall outside the limits of theoretical calculations. It may not be surprising if such a simple model fails to reproduce the experimental data quantitatively.

Recently a nuclear reaction code MAURINA [15] has been developed which also allows for the calculation of the isomeric yield ratio, and the present results are compared with model calculations performed with this code. The underlying model accounts in the first step for preequilibrium and equilibrium emissions. The former is treated in the frame of the exciton model. All further emissions of particles and photons are regarded as equilibrium compound nucleus evaporation. Earlier applications of the code and details of the above model can be found elsewhere [7,8]. We describe here very briefly some of the important model assumptions. In the calculations of emissions from the compound nucleus, the conservation of angular momentum and parity was taken into account thoroughly. The angular momentum effects during precompound emissions were considered in the present calculation using the "mean-lifetime ansatz" as proposed by Xiangjun, Gruppelaar, and Akkermans [33]. This can account for the angular momentum dependent competition between different decay modes. The choice of discrete nuclear levels at low excitation energies of the product nucleus was found [7,8] to be critical in the computation of isomeric yield ratios. They were taken from the recent compilation of Nuclear Data Sheets [34–37]. In the continuum region, the level density formula was derived from a combination of constant temperature form and the model of Kataria, Ramamurthy, and Kapoor [38]. In some cases, where ever possible, the level density parameters were based on experimental resonance spacings [39]. The spin distribution parameter of the level density is characterized by the ratio of the effective moment of inertia (θ_{eff}) to the rigid body moment of inertia (θ_{rig}): $\eta=e_{eff}/e_{rig}$. Since the spin distribution parameter should influence the isomer ratio values strongly, all calculations were performed for $\eta=1.0$ and 0.5.

To assess the reliability of the code MAURINA, at first total cross sections for all the reactions studied here were computed. The model was found to reproduce experimental excitation functions reasonably well. Theoretical predictions for isomeric yield ratios of ^{108}In, ^{110}In, ^{111}In, and ^{104}Ag for $\eta=0.5$ and 1.0 for all relevant nuclei are shown in Figs. 6 and 7 along with the experimental data. It appears that isomeric yield ratios for the ^{107}Ag$(\alpha,3n)$ and ^{107}Ag$(\alpha,\alpha 3n)$ reactions can be better described by $\eta=0.5$, while for the reactions on ^{109}Ag the choice of

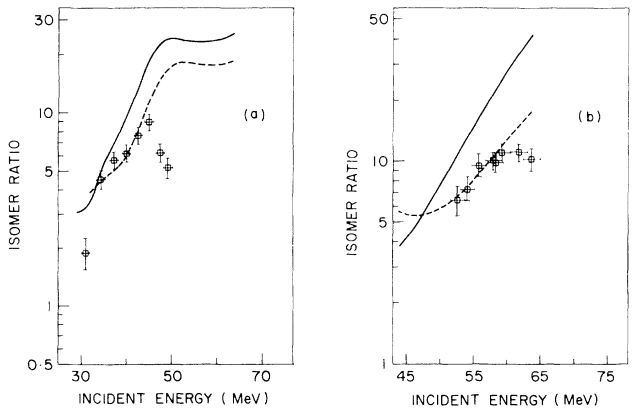

FIG. 6. Isomeric yield ratios as a function of incident energy of α particles (a) for the isomeric pair ^{108m,g}In in the reaction ^{107}Ag$(\alpha,3n)$ and (b) for the isomeric pair ^{104m,g}Ag in the reaction ^{107}Ag$(\alpha,\alpha 3n)$. Square points describe the experimental data, and curves represent the results of model calculations [15]. The solid line corresponds to $\eta=1.0$ and the dashed one to $\eta=0.5$.

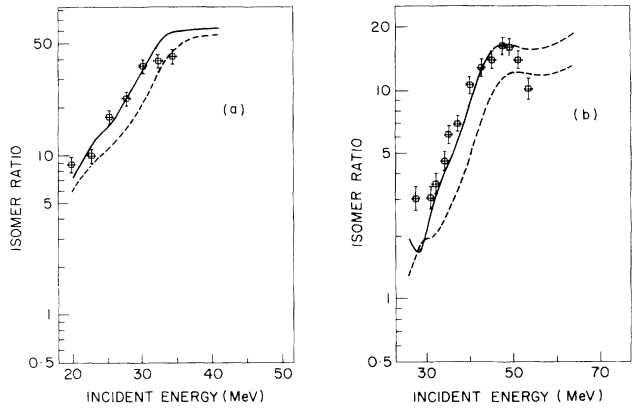

FIG. 7. Isomeric yield ratios as a function of incident energy of α particles (a) for the isomeric pair ^{111m,g}In in the reaction ^{109}Ag$(\alpha,2n)$ and (b) for the isomeric pair ^{110m,g}In in the reaction ^{109}Ag$(\alpha,3n)$. Other details are the same as for Fig. 6.

$\eta=1.0$ seems to be more reasonable. As expected, isomer ratios are found to depend strongly on the spin distribution parameter. However, in view of the uncertainties of the models and parameters, definite conclusions on the value of η are difficult. From Figs. 6 and 7, it is evident that theory predicts isomeric yield ratios fairly well for compound nuclear reactions. At higher bombarding energies when the preequilibrium particle emission becomes dominant, the theory predicts isomer ratios almost independent of the bombarding energy, whereas the experimental σ_{HS}/σ_{LS} values are found to decrease. A similar decrease in the isomeric yield ratio was also observed elsewhere [12]. The discrepancy observed at higher bombarding energies should be theoretically investigated in greater detail.

In conclusion, one can say that by using a global set of parameters a reasonable overall agreement between theory and experiment could be achieved for isomeric yield ratios. The method can therefore be possibly used with success for other reactions as well especially at low bombarding energy when the compound nuclear reaction channel is dominant.

ACKNOWLEDGMENTS

The authors thank Dr. R. M. Iyer, Chemical and Isotope Group, BARC, Dr. P. R. Natarajan, Radiochemistry Division, BARC, and Dr. B. C. Sinha, VECC, for their keen interest in this work. Thanks are also due to the operational staff of the cyclotron for providing us with irradiation facilities. All calculations employing the code MAURINA were performed on an IBM 3090-400E computer installed at the University of Vienna. We acknowledge this opportunity and the support of the Vienna University Computer Centre.

[1] M. Blann, Annu. Rev. Nucl. Sci. **25**, 123 (1975), and references therein.
[2] F. Puhlhofer, Nucl. Phys. **A280**, 267 (1977).
[3] E. Gadioli, E. Gadioli-Erba, and J. J. Hogan, Phys. Rev. C **16**, 1404 (1977).
[4] S. A. Hjorth, H. Ryde, K. A. Hagemann, G. Lovhoiden, and J. C. Waddington, Nucl. Phys. **A144**, 513 (1970).
[5] J. Ernst, R. Ibowski, H. Klampil, H. Machner, T. Mayer-Kuckuk, and R. Shanz, Z. Phys. A **308**, 301 (1982).
[6] M. Ismail, Phys. Rev. C **41**, 87 (1990).
[7] S. M. Qaim, A. Mushtaq, and M. Uhl, Phys. Rev. C **38**, 645 (1988).
[8] N. I. Molla, S. M. Qaim, and M. Uhl, Phys. Rev. C **42**, 1540 (1990).
[9] C. T. Bishop, J. R. Huizenga, and J. P. Hummel, Phys. Rev. **135**, B401 (1964).
[10] K. J. Moody and J. J. Hogan, Phys. Rev. C **34**, 899 (1986).
[11] I. S. Grant and M. Rathle, J. Phys. G **5**, 1741 (1979).
[12] S. K. Saha, R. Guin, and S. M. Sahakundu, J. Radioanal. Nucl. Chem. Lett. **119**, 303 (1987).
[13] G. W. A. Newton, V. J. Robinson, and E. M. Shaw, J. Inorg. Nucl. Chem. **43**, 2227 (1981).
[14] M. Blann, ALICE/85/300, LLNL Report No. UCID 20169, 1984, and references therein.
[15] M. Uhl (unpublished).
[16] C. F. Williamson, J. P. Boujot, and J. Pickard, Commissariat à l'Energie Atomique (France) Report No. CEA-R 3042, 1966.
[17] H. J. Probst, S. M. Qaim, and R. Weinreich, Int. J. Appl. Radiat. Isot. **27**, 431 (1976).
[18] R. Guin, S. K. Saha, S. M. Sahakundu, and Satya Prakash, J. Radioanal. Nucl. Chem. Artic. **141**, 185 (1990).
[19] C. M. Lederer and V. S. Shirley, *Tables of Isotopes*, 7th ed. (Wiley, New York, 1978).
[20] R. Guin, Ph.D. thesis, University of Bombay, India, 1990.
[21] S. Fukushima, S. Hayashi, S. Kume, H. Okamura, K. Otozai, K. Sakamoto, and Y. Yoshizawa, Nucl. Phys. **41**, 275 (1963).

[22] S. Fukushima, S. Kume, H. Okamura, K. Otozai, K. Sakamoto, and Y. Yoshizawa, Nucl. Phys. **69**, 273 (1965).
[23] P. Misaelides and H. Munzel, J. Inorg. Nucl. Chem. **42**, 937 (1980).
[24] C. Wasilevsky, M. De la Vega Vedoya, and S. J. Nassif, J. Radional. Nucl. Chem. Artic. **89**, 531 (1985).
[25] C. Wasilevsky, M. De la Vega Vedoya, and S. J. Nassif, J. Radioanal. Nucl. Chem. Lett. **95**, 29 (1985).
[26] M. Blann, Phys. Rev. Lett. **27**, 337 (1971).
[27] C. K. Cline and M. Blann, Nucl. Phys. **A172**, 225 (1971).
[28] J. J. Griffin, Phys. Rev. Lett. **17**, 478 (1966).
[29] G. D. Harp, J. M. Miller, and J. B. Berne, Phys. Rev. **165**, 1166 (1968).
[30] G. D. Harp and J. M. Miller, Phys. Rev. C **3**, 1847 (1971).
[31] W. D. Myers and W. J. Swiatecki, Ark. Fys. **36**, 343 (1967).
[32] A. Chevarier, N. Chevarier, A. Demeyer, G. Hollinger, P. P. Pertosa, and T. M. Duc, Phys. Rev. C **8**, 2155 (1973).
[33] Shi Xiangjun, H. Gruppelaar, and J. M. Akkermans, Nucl. Phys. **A466**, 333 (1987).
[34] J. Blachot, J. P. Husson, J. Omes, and G. Berrier, Nucl. Data Sheets **41**, 325 (1984).
[35] B. Harmatz, Nucl. Data Sheets **27**, 453 (1979).
[36] P. De Gelder, E. Jacobs, and D. De Franne, Nucl. Data Sheets **38**, 545 (1983).
[37] R. L. Haese, F. E. Bertrand, B. Harmatz, and M. J. Martin, Nucl. Data Sheets **37**, 289 (1982).
[38] S. K. Kataria, V. S. Ramamurthy, and S. S. Kapoor, Phys. Rev. C **18**, 549 (1978).
[39] S. F. Mughabghab, M. Divadeenam, and N. E. Holden, *Neutron Cross Sections* (Academic, New York, 1981), Vol. I, Part A.